

Strain-specific and tissue-specific expression of mouse mast cell secretory granule proteases

RICHARD L. STEVENS*^{†‡}, DANIEL S. FRIEND*[§], H. PATRICK MCNEIL*[†], VERA SCHILLER[†],
NAMIT GHILDYAL*[†], AND K. FRANK AUSTEN*[†]

*Department of Medicine, Harvard Medical School, and Departments of [†]Rheumatology and Immunology and [§]Pathology, Brigham and Women's Hospital, Boston, MA 02115

Contributed by K. Frank Austen, August 23, 1993

ABSTRACT As assessed by RNA blot analyses with gene-specific probes, we report that the perivascular connective tissue mast cells (CTMCs) in the ear and skin of BALB/cJ mice contain abundant levels of the mouse mast cell protease (mMCP) 7 transcript, in addition to those protease transcripts present in their serosal mast cells (SMCs). High levels of the mMCP-7 transcript also were detected in the ears of WBB6F₁/J-+/, WCB6F₁/J-+/, WB/ReJ-+/, and WC/ReJ-+/+ mice. However, the ears of these four strains and the SMCs from the WCB6F₁/J-+/+ strain but not the BALB/cJ strain also contained high steady-state levels of the mMCP-2 transcript. The mMCP-2, mMCP-4, mMCP-5, mMCP-6, and mMCP-7 transcripts were not detected in the ears of mast-cell-deficient WBB6F₁/J-W/W^v and WCB6F₁/J-SI/SI^d mice, indicating that mast cells were the source of these protease transcripts in the +/+ animals. When immunohistochemical analyses of serial sections of ear and skin from WBB6F₁/J-+/+ mice were performed with anti-mMCP-2 IgG and anti-mMCP-5 IgG, the perivascular CTMCs in these tissues were found to express both mMCP-2 and mMCP-5 in their granules. The prominent expression of mMCP-7 in constitutive perivascular CTMCs indicates that this mast cell has an extended protease phenotype relative to the SMCs of the same strains. Further, the perivascular CTMCs and SMCs of the +/+ strains differ from those in BALB/cJ mice in their prominent expression of mMCP-2.

As assessed by protein sequencing and/or by cDNA cloning, mouse mast cells differentiated *in vivo* and *in vitro* express varied combinations of carboxypeptidase A (mMC-CPA) (1) and at least seven serine proteases [designated mouse mast cell protease (mMCP) 1 to mMCP-7] in their granules (2–11). The safranin⁺ staining serosal mast cells (SMCs) of the BALB/cJ mouse contain high steady-state levels of the transcripts that encode mMCP-4, mMCP-5, and mMCP-6 but not mMCP-1, mMCP-2, or mMCP-7. In contrast, the safranin⁻ mucosal mast cells that proliferate in the intestine of helminth-infected BALB/cJ mice contain high steady-state levels of the mMCP-1 and mMCP-2 transcripts but not the mMCP-4, mMCP-5, mMCP-6, or mMCP-7 transcripts. Although these two histochemically distinct populations of tissue mast cells apparently express their granule proteases in a strict subclass-specific manner, nontransformed but immature populations of BALB/cJ mouse mast cells derived *in vitro* can express varied combinations of the eight mMCPs in response to different recombinant cytokines (12–16).

In this study, we have used RNA blot and RNase protection analyses to demonstrate a third population of mast cells *in situ* in BALB/cJ mice, namely, a population of perivascular connective tissue mast cells (CTMCs) that expresses prominent steady-state levels of the mMCP-7 transcript in

addition to those protease transcripts expressed by SMCs. We also present RNA and immunohistochemical data that indicate that the WBB6F₁/J-+/, WCB6F₁/J-+/, WB/ReJ-+/, and WC/ReJ-+/+ strains of mice differ from the BALB/cJ mouse strain in their prominent expression of mMCP-2 in both their SMCs and perivascular CTMCs.

MATERIALS AND METHODS

Mouse Mast-Cell-Specific Protease mRNA Levels in Ear and Skin CTMCs and Isolated SMCs. Female mice of the WB/ReJ-+/, WC/ReJ-+/+, WBB6F₁/J-+/, WCB6F₁/J-+/, WBB6F₁/J-W/W^v, WCB6F₁/J-SI/SI^d, and BALB/cJ strains (The Jackson Laboratory) were killed by cervical dislocation, and their ears and/or abdominal skin were removed and placed in liquid nitrogen for RNA isolation. Ears from three to six mice of the same strain were pooled, ground in liquid nitrogen with a mortar and pestle, and homogenized briefly in 4 M guanidinium thiocyanate/0.5% sarcosyl/0.1 M 2-mercaptoethanol/25 mM sodium citrate. SMCs were isolated from BALB/cJ mice and WBB6F₁/J-+/+ mice by peritoneal lavage of the animals (17) and purified by density-gradient centrifugation of the cells obtained (18). Total (19) and/or poly(A)⁺ (20) RNAs were isolated from the various ear, skin, and SMC samples, denatured in formaldehyde/formamide, electrophoresed in 1.3% formaldehyde/agarose gels, and transferred to MagnaGraph membranes (Micron Separations, Westover, MA) (21). The resulting blots were analyzed sequentially with gene-specific probes for mMCP-1 (8, 14), mMCP-2 (3), mMCP-5 (7), mMCP-6 (5), mMCP-7 (9), mMC-CPA (1), and β -actin (22) and with a gene-selective probe for mMCP-4 (6). An RNase protection assay (14) was performed with a kit from Ambion (Austin, TX), [³²P]dUTP-labeled (DuPont/New England Nuclear) complementary RNA probes, and $\approx 2.5 \mu\text{g}$ of poly(A)⁺ RNA from the ear and skin of WCB6F₁/J-+/+ mice and WCB6F₁/J-SI/SI^d mice. The mMCP-2, mMCP-4, mMCP-5, and mMCP-7 complementary RNA antisense probes corresponded to the residues 804–956, 497–633, 768–972, and 854–1021 of their respective cDNAs. The protected RNA fragments were resolved on a 6% polyacrylamide/8 M urea sequencing gel and analyzed by autoradiography.

Histochemistry and Immunohistochemistry of Mouse Ear and Skin CTMCs. For histological examination, 2- μm -thick glycol methacrylate sections of ear and back skin from BALB/cJ, WBB6F₁/J-+/, and WBB6F₁/J-W/W^v mice were cut on a Reichert–Jung model 2065 supercut rotary microtome (Leica, Deerfield, IL), placed on coverslips or slides, air-dried, and stained for 20 s in a 5% (wt/vol)

ethanolic solution of methylene blue (23) or stained sequentially with hematoxylin, azure II, and eosin Y (24). For immunoperoxidase and immunoalkaline phosphatase labeling, coverslips supporting 2- μ m-thick serial sections of glycol methacrylate-embedded Carnoy's-fixed ear and back skin from BALB/cJ and WBB6F₁/J-+/+ mice were incubated for 10 min at 37°C in phosphate-buffered saline (PBS) containing 0.25% trypsin. The samples were washed with 0.2% Tween 20, incubated for 30 min at 37°C in PBS containing 0.05% Tween 20 and 4% (vol/vol) goat serum, and then incubated overnight at 4°C with affinity-purified rabbit anti-mMCP-2 IgG (epitope, residues 56-71) (15) or anti-mMCP-5 IgG (epitope, residues 146-162) (25) diluted in goat serum. The samples were washed, incubated for 1 h at room temperature in buffer containing biotin-labeled goat anti-rabbit IgG, and washed again. Endogenous peroxidase was eliminated before the diaminobenzidine reaction by incubating the samples in 0.3% H₂O₂/30% (vol/vol) methanol or in 0.23% periodic acid. Before the alkaline phosphatase reaction product was developed, the tissues were washed in 0.1% bovine serum albumin/0.05% Tween 20 in PBS. After another wash, the samples were incubated in the peroxidase or alkaline phosphatase Vectastain ABC reagent (Vector Laboratories) for 30 min at room temperature. The developing peroxidase reaction was carried out for 10 min in the dark in 10 ml of PBS containing 5 mg of diaminobenzidine and 0.125 g of imidazole. H₂O₂ (0.01%) was added, and the sections were incubated for another 15 min in the dark. The developing alkaline phosphatase substrate was used according to directions in the Vectastain kit. Because of the melanocytes in the skin of the WBB6F₁/J-+/+ mouse, the red alkaline phosphatase reaction product is depicted in the figures to distinguish the reporter color from the endogenous brown melanin pigment. Sections were counterstained with equal volumes of hematoxylin 3 and 20% (vol/vol) ethylene glycol, washed, dried, and mounted with Permount for the peroxidase reaction product and Equamount (Shandon-Lipshaw, Pittsburgh) for alkaline phosphatase reaction product. Controls consisted of sections treated without primary antibodies, with IgG preabsorbed with a relevant blocking peptide, or with an irrelevant IgG (Endogen, Boston). Twelve sets of serial sections of ear and six sets of serial sections of back skin were examined for reactivity with anti-mMCP-2 IgG (15) and anti-mMCP-5 IgG (25).

RESULTS

Mouse Mast-Cell-Specific Protease mRNA Levels in Ear and Skin CTMCs and Isolated SMCs. As assessed by RNA blot analysis, the ears of BALB/cJ mice ($n = 5$) (Fig. 1A) contained abundant levels of the transcripts that encode mMCP-4, mMCP-5, mMCP-6, mMCP-7, and mMC-CPA but not mMCP-1 or mMCP-2. No substantial difference was noted in the steady-state levels of these different mast cell protease transcripts in the ears of 9-week-old BALB/cJ mice vs. retired BALB/cJ breeders (data not shown) ($n = 1$). Because no mature mast cell has been found that expresses abundant levels of the mMCP-7 transcript and to ensure that the mMCP-7 transcript originated from the mast cells in the ear, the levels of the seven protease transcripts were evaluated in the ears of two mast-cell-deficient strains, their +/+ littermates, and related ReJ-+/+ strains. As assessed by RNA blot analysis, the ears of WBB6F₁/J-+/+ ($n = 5$), WCB6F₁/J-+/+ ($n = 5$), WB/ReJ-+/+ ($n = 1$), and WC/ReJ-+/+ ($n = 1$) mice contained abundant levels of the transcripts that encode mMCP-2, mMCP-4, mMCP-5, mMCP-6, and mMCP-7 but not mMCP-1 (Fig. 1). Since none of these protease transcripts was detected in the ears of mast-cell-deficient WBB6F₁/J-W/W^v mice ($n = 5$) or WCB6F₁/J-SI/SI^d mice ($n = 5$) (Fig. 1B), it is likely that they

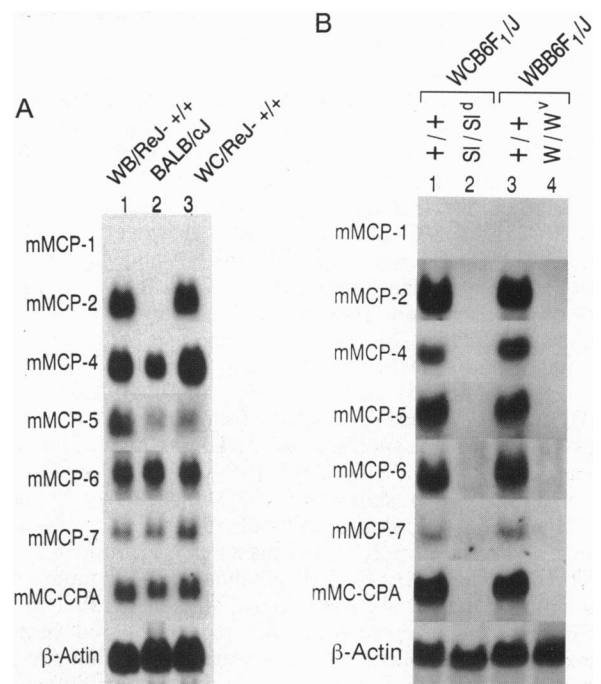


Fig. 1. Steady-state levels of mast-cell-specific protease transcripts in mouse ears. The blots (A and B), containing total RNA from the ears of the indicated mice, were analyzed with the designated probes.

all originated from the safranin⁺ mast cells in the tissues of the +/+ mice. Whereas the perivascular CTMCs in the ears of all five strains contained high steady-state levels of mMCP-7 mRNA, the prominent steady-state level of the mMCP-2 transcript appeared to be strain-dependent.

To ensure that the results of the RNA blot analyses were not consequences of cross hybridization of the mMCP-2, mMCP-4, mMCP-5, and mMCP-7 cDNAs to homologous transcripts and to determine whether perivascular CTMCs in other tissues express these transcripts, a RNase protection experiment was performed with poly(A)⁺ RNA isolated from the ear and skin of WCB6F₁/J-+/+ mice and WCB6F₁/J-SI/SI^d mice. Poly(A)⁺ RNA from both the skin and the ear of the WCB6F₁/J-+/+ mouse protected the mMCP-2, mMCP-4, mMCP-5, and mMCP-7 probes from degradation (Fig. 2). In contrast, poly(A)⁺ RNA from the skin and ear of

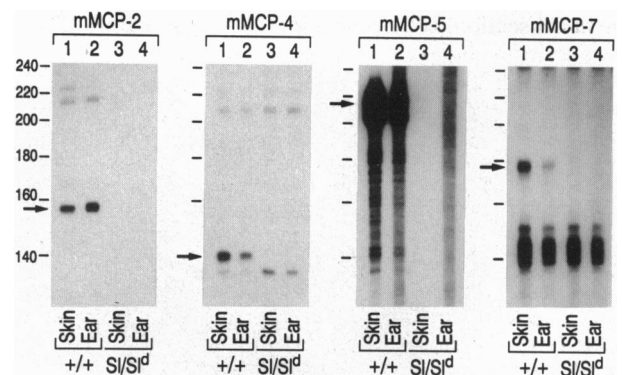


Fig. 2. RNase protection analyses. The presence or absence of the transcripts that encode mMCP-2, mMCP-4, mMCP-5, and mMCP-7 was assessed with antisense complementary RNA probes and RNA isolated from the skin (lanes 1 and 3) and ears (lanes 2 and 4) of WCB6F₁/J-+/+ mice (lanes 1 and 2) and WCB6F₁/J-SI/SI^d mice (lanes 3 and 4). The arrows indicate the sizes of the probes that were expected to be protected if the specific transcript was present in the sample.

the mast-cell-deficient WCB6F₁/J-*Sl/Sl*^d mouse failed to protect these probes from degradation.

RNA blot analysis revealed that isolated SMCs from BALB/cJ mice contained high steady-state levels of the mMCP-4 and mMC-CPA transcripts, barely detectable levels of the mMCP-7 transcript, and no detectable amount of the mMCP-2 transcript (Fig. 3). SMCs isolated from WBB6F₁/J-+/+ mice also contained high steady-state levels of the mMCP-4 and mMC-CPA transcripts. However, they contained a very high level of mMCP-2 mRNA and slightly more mMCP-7 mRNA than SMCs isolated from BALB/cJ mice.

Histochemistry and Immunohistochemistry of Mouse Ear and Skin CTMCs. Morphometric analysis of the >1000 methylene blue⁺ mast cells detected in 2- μ m-thick sections of ear (Figs. 4 and 5) and skin (Fig. 6) of BALB/cJ and WBB6F₁/J-+/+ mice revealed the following number of mast cells per mm² of tissue: ears of BALB/cJ mice, 106 \pm 30 (mean \pm SD, *n* = 3); ears of WBB6F₁/J-+/+ mice, 85 \pm 27 (mean \pm SD, *n* = 4); skin of BALB/cJ mice, 100 \pm 19 (mean \pm 1/2 range, *n* = 2); skin of WBB6F₁/J-+/+ mice, 84 \pm 11 (mean \pm 1/2 range, *n* = 2). Only 1 mast cell was found in 8 mm² of skin from the WBB6F₁/J-*W/W*^v mouse. In the mouse ear, most of the mast cells were found aligned parallel to the cartilage plates in close proximity to small blood vessels, nerves, and fibroblasts. A few were found immediately beneath the squamous epithelium. In the skin of the mouse, some mast cells were detected beneath the basal layer of epithelium, but most were found enmeshed in collagen near small blood vessels, nerves, fibroblasts, and adipocytes.

In a representative experiment, 138 methylene blue⁺ mast cells were detected in a section of a WBB6F₁/J-+/+ mouse ear. Analysis of comparable-sized sections from the same specimen revealed 135 cells that reacted strongly with anti-mMCP-2 IgG, 130 cells that reacted strongly with anti-mMCP-5 IgG, and 5 cells that reacted weakly when no primary antibody was used (data not shown). In four experiments, 86 \pm 11% (mean \pm SD) of the mast cells in the ears of this strain expressed mMCP-2 and 93 \pm 11% expressed mMCP-5. Analysis of a section of BALB/cJ mouse ear processed at the same time revealed 229 methylene blue⁺ mast cells. In comparable-sized sections from the same specimen, 177 cells reacted strongly with anti-mMCP-5 IgG, 51 reacted weakly with anti-mMCP-2 IgG, and 7 cells reacted weakly when no primary antibody was used (Fig. 5). In another experiment, 88% of the mast cells reacted strongly with anti-mMCP-5 IgG, 13% reacted weakly with anti-mMCP-2 IgG, and 3% reacted weakly when no primary antibody was used. Serial sections of ear (data not shown) and serial sections of skin (Fig. 6) from the WBB6F₁/J-+/+

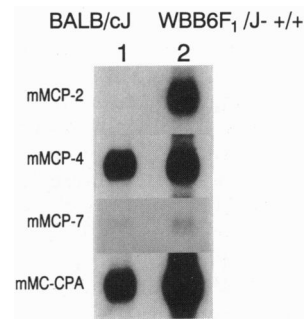


FIG. 3. Steady-state levels of mast-cell-specific proteases in isolated SMCs. The blot containing total RNA from BALB/cJ (lane 1) and WBB6F₁/J-+/+ (lane 2) mouse SMCs was analyzed with the indicated probes. In a second experiment, abundant amounts of the mMCP-2 transcript were again detected in the SMCs from the +/+ mice but not BALB/cJ mice.

mouse were examined with anti-mMCP-2 IgG and anti-mMCP-5 IgG for individual cells that express both mMCP-2 and mMCP-5. As assessed immunohistochemically, a typical $\times 20$ objective microscopic field of a 2- μ m-thick section of skin from a WBB6F₁/J-+/+ mouse contained 15 cells that expressed immunoreactive mMCP-5; 7 of these specific mast cells in the adjacent 2- μ m section also expressed immunoreactive mMCP-2. The mast cells immediately beneath the stratified squamous epithelium generally were less reactive to anti-mMCP-2 IgG than the mast cells that resided deep in the dermis. In the ear, similar consecutively sectioned fields typically contained 28 mast cells, two-thirds of which expressed both serine proteases.

DISCUSSION

This study shows that the perivascular CTMCs in the ears and skin of the BALB/cJ mouse express prominent steady-state levels of mMCP-7 transcript, thereby distinguishing this population from SMCs and mucosal mast cells of the same strain. This study also shows that the SMCs and perivascular CTMCs of +/+ mice prominently express mMCP-2 while those in BALB/cJ mice do not, thereby establishing a strain-dependent difference in the expression of a granule constituent.

SMCs from BALB/cJ mice preferentially express mMCP-4, mMCP-5, mMCP-6, and mMC-CPA (1, 4-7), whereas the mast cells that proliferate in the intestines of helminth-infected BALB/cJ mice preferentially express mMCP-1 and mMCP-2 (2, 14, 15). RNA blot analyses (Fig.

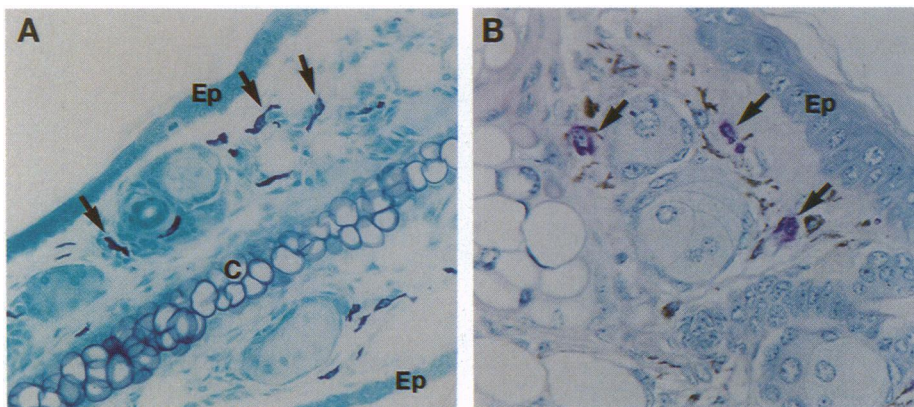


FIG. 4. (A) A 2- μ m-thick cross-section of a BALB/cJ mouse ear was stained with methylene blue. Arrows indicate three CTMCs (among 12 cells) between the cartilage (C) and squamous epithelium (Ep). Mast-cell density is greater around glands, hair follicles, and blood vessels. (B) A comparable section of a WBB6F₁/J-+/+ mouse ear stained with hematoxylin, azure II, and eosin. Mast cells (arrows) stain purple. The brown cells are melanin⁺ melanocytes.

1A) revealed that the ears of BALB/cJ mice contained high steady-state levels of the transcripts that encode mMCP-4, mMCP-5, mMCP-6, mMCP-7, and mMC-CPA but not mMCP-1 or mMCP-2. Although certain immature interleukin (IL) 3-dependent mouse bone-marrow-derived mast cells and certain transformed mast cell lines such as Abelson virus-immortalized mast cells express mMCP-7 (9), to our knowledge, no population of *in vivo*-derived mast cells has been previously recognized to contain high steady-state levels of this tryptase transcript. RNA blot analyses of the ears of WBB6F₁/J-+/+, WCB6F₁/J-+/+, WB/ReJ-+/+, and WC/ReJ-+/+ mice revealed that these four strains contained high steady-state levels of the mMCP-2 transcript, in addition to the mMCP-4, mMCP-5, mMCP-6, mMCP-7, and mMC-CPA transcripts (Fig. 1). RNase protection analysis confirmed that the perivascular CTMCs in the skin of a +/+ mouse express mMCP-2 and mMCP-7 (Fig. 2). No mMCP transcript was detected in the RNA samples obtained from the mast-cell-deficient mouse strains (Fig. 1B), and poly(A)⁺ RNA isolated from the ear and skin of the WCB6F₁/J-SI/SI^d mouse failed to protect the mMCP-2, mMCP-4, mMCP-5, and mMCP-7 probes from degradation (Fig. 2). Thus, the methylene blue⁺ (Fig. 4) mast cells in the ear and skin of the +/+

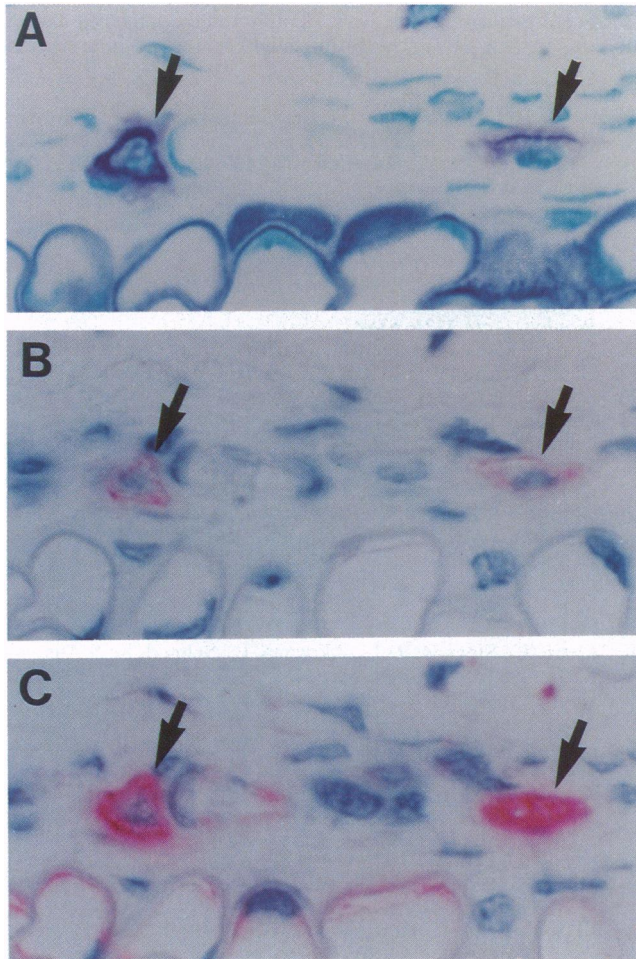


FIG. 5. Two mast cells (arrows) in serial sections of an ear from a BALB/cJ mouse stained with methylene blue (A), anti-mMCP-2 IgG (B), and anti-mMCP-5 IgG (C). In this mouse strain, the amount of alkaline phosphatase reaction product formed with anti-mMCP-2 IgG in cells that we scored positive is considerably less than that obtained with anti-mMCP-5 IgG. In some instances, the intensity of the reaction is comparable to that of sections not exposed to primary antibody.

mice are the source of the transcripts for mMCP-2, mMCP-4, mMCP-5, mMCP-6, mMCP-7, and mMC-CPA.

The failure to detect mMCP-1 mRNA (Fig. 1) indicates that classical mucosal mast cells are not present in these connective tissues. The abundance of the mMCP-7 transcript in ear and skin mast cells is additional evidence that the RNA blot analyses are not a composite of the known separate SMCs and mucosal mast cell phenotypes in the BALB/cJ mouse. The safranin⁺ KiSV-MC5 cell line, which has been maintained in continuous culture for 5 years, contains high steady-state levels of the mMCP-2, mMCP-4, mMCP-5, and mMCP-6 transcripts, lower levels of the mMCP-7 transcript, and undetectable levels of the mMCP-1 transcript (1, 3–7, 9, 15). As with *in vitro*-differentiated cells (4, 12–16), the data obtained in this study on *in vivo*-differentiated mast cells indicate that the ability of a mast cell to be stained by safranin does not define its protease phenotype. Whether or not a mast cell is safranin⁺ appears to be determined almost exclusively by its heparin content, and the biosynthesis of heparin is differentially regulated from most of the secretory granule proteases (12, 18).

As was found (1, 3–7), the SMCs of BALB/cJ mice contained high steady-state levels of the transcripts that encode mMCP-4 and mMC-CPA but not mMCP-2 or mMCP-7 (Fig. 3). SMCs from the WBB6F₁/J-+/+ strain differed in that they contained high steady-state levels of the mMCP-2 transcript and low levels of the mMCP-7 transcript. Thus, the SMCs in this strain are similar to the CTMCs in ear and skin in terms of their steady-state levels of the mMCP-2 transcript but differ in regard to the mMCP-7 transcript.

The profile of the ear and skin perivascular CTMCs of one of the +/+ strains was confirmed at the protein level by the immunohistochemical detection of both mMCP-2 and mMCP-5 in the same cell. As assessed immunohistochemically in the WBB6F₁/J-+/+ mouse, at least 85% of the ear (data not shown) and skin (Fig. 6) CTMCs react strongly with anti-mMCP-5 IgG and anti-mMCP-2 IgG. The concomitant expression of mMCP-2 and mMCP-5 was demonstrated in one-half to two-thirds of the mast cells in adjacent serial sections of the ear and skin. If the thickness of the sections is considered relative to the size of the mast cell, this result is compatible with most of the perivascular CTMCs in the WBB6F₁/J-+/+ mouse strain expressing both proteases. Not only was the intensity of the immunohistochemical reaction for mMCP-2 notably less in the BALB/cJ strain relative to the +/+ strain (Fig. 5), but only a net of ≈15% of the CTMCs in the ears of the BALB/cJ mouse were immunoreactive. Although the RNA blot analyses indicated that the skin and ears of the adult BALB/cJ mouse do not contain high steady-state levels of the mMCP-2 transcript, a minor population of mast cells in these tissues may contain a low amount of mMCP-2 mRNA. Since the kinetics of loss of mMCP-2 protein is slowed relative to that of the mMCP-2 transcript in IL-10-treated BALB/cJ bone marrow-derived mast cells that are subsequently cultured in medium lacking IL-10 (15), an alternative explanation would be that progenitor mast cells that home to the ear and skin of the BALB/cJ mice transiently express high steady-state levels of the mMCP-2 transcript.

The factors that induce the expression of mMCP-7 in the mast cells of the ear and skin of all strains studied and suppress the expression of mMCP-2 in the BALB/cJ strain are unknown. The strain dependence of mMCP-2 expression was unexpected because the mucosal mast cells that increase in the intestines of helminth-infected BALB/cJ mice express mMCP-2 (14, 15), and mouse bone marrow-derived mast cells derived from this strain express mMCP-2 when they are cultured with IL-10 (13, 15) or IL-9 (16). Thus, the mast-cell-committed progenitor cells in BALB/cJ mice do not have a genetic inability to elicit expression of mMCP-2. Since ke-

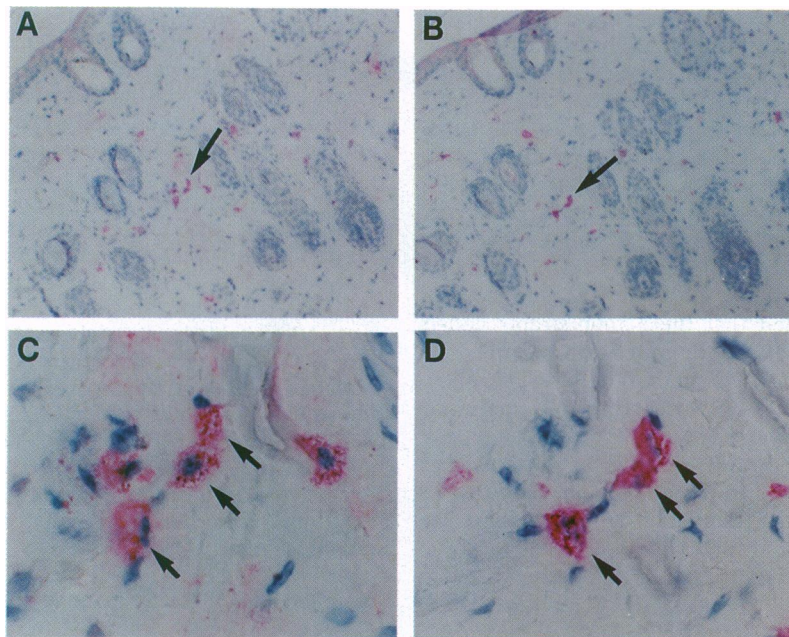


FIG. 6. Serial sections of skin from a WBB6F₁/J-+/+ mouse stained with anti-mMCP-2 IgG (A and C) or with anti-mMCP-5 IgG (B and D). In the low magnification views (A and B), arrows indicate serially sectioned cells that can be positively identified as the same cell having the red alkaline phosphatase reaction product. C and D are higher magnifications of the same fields. The arrows indicate three cells that contain immunoreactive mMCP-2 and mMCP-5.

ratinocytes produce IL-10 (26), it is possible that IL-10 or another mMCP-2-inducing cytokine is constitutively overexpressed in the +/+ mouse strains relative to the BALB/cJ mouse strain. Whatever the mechanism, the strain-dependent expression of mMCP-2 indicates that WBB6F₁/J-+/+ and WBB6F₁/J-+/+ mice can no longer be considered analogous to all other strains of mice in terms of their granule constituents. The finding that in BALB/cJ mice the steady-state level of the mMCP-7 transcript is considerably higher in its perivascular CTMCs than in its SMCs also indicates that not all safranin⁺ mast cells in this strain are identical in terms of their granule constituents.

The comments of Dr. H. Katz (Harvard Medical School) who reviewed this manuscript are gratefully acknowledged. This work was supported by Grants AI-22531, AI-23483, AI-31599, AR-36308, GM-46697, HG-00189, and HL-36110 from the National Institutes of Health and by a grant from the Hyde and Watson Foundation.

1. Reynolds, D. S., Stevens, R. L., Gurley, D. S., Lane, W. S., Austen, K. F. & Serafin, W. E. (1989) *J. Biol. Chem.* **264**, 20094–20099.
2. Le Trong, H., Newlands, G. F. J., Miller, H. R. P., Charbonneau, H., Neurath, H. & Woodbury, R. G. (1989) *Biochemistry* **28**, 391–395.
3. Serafin, W. E., Reynolds, D. S., Rogelj, S., Lane, W. S., Conder, G. A., Johnson, S. S., Austen, K. F. & Stevens, R. L. (1990) *J. Biol. Chem.* **265**, 423–429.
4. Reynolds, D. S., Stevens, R. L., Lane, W. S., Carr, M. H., Austen, K. F. & Serafin, W. E. (1990) *Proc. Natl. Acad. Sci. USA* **87**, 3230–3234.
5. Reynolds, D. S., Gurley, D. S., Austen, K. F. & Serafin, W. E. (1991) *J. Biol. Chem.* **266**, 3847–3853.
6. Serafin, W. E., Sullivan, T. P., Conder, G. A., Ebrahimi, A., Marcham, P., Johnson, S. S., Austen, K. F. & Reynolds, D. S. (1991) *J. Biol. Chem.* **266**, 1934–1941.

7. McNeil, H. P., Austen, K. F., Somerville, L. L., Gurish, M. F. & Stevens, R. L. (1991) *J. Biol. Chem.* **266**, 20316–20322.
8. Huang, R., Blom, T. & Hellman, L. (1991) *Eur. J. Immunol.* **21**, 1611–1621.
9. McNeil, H. P., Reynolds, D. S., Schiller, V., Ghildyal, N., Gurley, D. S., Austen, K. F. & Stevens, R. L. (1992) *Proc. Natl. Acad. Sci. USA* **89**, 11174–11178.
10. Johnson, D. A. & Barton, G. J. (1992) *Protein Sci.* **1**, 370–377.
11. Chu, W., Johnson, D. A. & Musich, P. R. (1992) *Biochim. Biophys. Acta* **1121**, 83–87.
12. Gurish, M. F., Ghildyal, N., McNeil, H. P., Austen, K. F., Gillis, S. & Stevens, R. L. (1992) *J. Exp. Med.* **175**, 1003–1012.
13. Ghildyal, N., McNeil, H. P., Gurish, M. F., Austen, K. F. & Stevens, R. L. (1992) *J. Biol. Chem.* **267**, 8473–8477.
14. Ghildyal, N., McNeil, H. P., Stechschulte, S., Austen, K. F., Silberstein, D., Gurish, M. F., Somerville, L. L. & Stevens, R. L. (1992) *J. Immunol.* **149**, 2123–2129.
15. Ghildyal, N., Friend, D. S., Nicodemus, C. F., Austen, K. F. & Stevens, R. L. (1993) *J. Immunol.* **151**, 3206–3214.
16. Eklund, K. K., Ghildyal, N., Austen, K. F. & Stevens, R. L. (1993) *J. Immunol.* **151**, 4266–4273.
17. Yurt, R. W., Leid, R. W., Jr., Austen, K. F. & Silbert, J. E. (1977) *J. Biol. Chem.* **252**, 518–521.
18. Razin, E., Stevens, R. L., Akiyama, F., Schmid, K. & Austen, K. F. (1982) *J. Biol. Chem.* **257**, 7229–7236.
19. Chomczynski, P. & Sacchi, N. (1987) *Anal. Biochem.* **162**, 156–159.
20. Aviv, H. & Leder, P. (1972) *Proc. Natl. Acad. Sci. USA* **69**, 1408–1412.
21. Thomas, P. S. (1980) *Proc. Natl. Acad. Sci. USA* **77**, 5201–5205.
22. Spiegelman, B. M., Frank, M. & Green, H. (1983) *J. Biol. Chem.* **258**, 10083–10089.
23. Matin, R., Tam, E. K., Nadel, J. A. & Caughey, G. H. (1992) *J. Histochem. Cytochem.* **40**, 781–786.
24. Beckstead, J. H., Halverson, P. S., Ries, C. A. & Bainton, D. F. (1981) *Blood* **57**, 1088–1098.
25. McNeil, H. P., Frenkel, D. P., Austen, K. F., Friend, D. S. & Stevens, R. L. (1992) *J. Immunol.* **149**, 2466–2472.
26. Enk, A. H. & Katz, S. I. (1992) *J. Immunol.* **149**, 92–95.